Co-delivery of a RanGTP inhibitory peptide and doxorubicin using dual loaded liposomal carriers to combat chemotherapeutic resistance in breast cancer cells

Yusuf Haggag , Bayan Abu Ras , Yahia El-Tanani , Murtaza M. Tambuwala , Paul McCarron , Mohammed Isreb & Mohamed El-Tanani

Accepted author version posted online: 25 Aug 2020.

Submit your article to this journal ↗

View related articles ↗

View Crossmark data ↗

Co-delivery of a RanGTP inhibitory peptide and doxorubicin using dual loaded liposomal carriers to combat chemotherapeutic resistance in breast cancer cells

Yusuf Haggag[1], Bayan Abu Ras[2], Yahia El-Tanani[2], Murtaza M. Tambuwala[3], Paul McCarron[3], Mohammed Isreb[2] and Mohamed El-Tanani[4,5]*

[1] Department of Pharmaceutical Technology, Faculty of Pharmacy, Tanta University, Tanta, Egypt.

[2] School of Pharmacy and Clinical Sciences, University of Bradford, Bradford BD7 1DP, UK.

[3] School of Pharmacy and Pharmaceutical Sciences, Ulster University, Cromore Road, Coleraine, Co. Londonderry, BT52 1SA, UK.

[4] Pharmacological and Diagnostic Research Centre, Al-Ahliyya Amman University, Faculty of Pharmacy, Amman, Jordan.

[5] Institute of Cancer Therapeutics, Faculty of Life Sciences, University of Bradford, Bradford BD7 1DP, UK.

*Correspondence

Mohamed El-Tanani

Pharmacological and Diagnostic Research Centre, Al-Ahliyya Amman University,

Faculty of Pharmacy, Amman, Jordan

Tel: 00962 788240945

Email: m.tanani@ammanu.edu.jo

Abstract

Background: Multidrug resistance (MDR) limits the beneficial outcomes of conventional breast cancer chemotherapy. Ras-related nuclear protein (Ran-GTP) plays a key role in these resistance mechanisms, assisting cancer cells to repair damage to DNA. Herein, we investigate the co-delivery of Ran-RCC1 inhibitory peptide (RAN-IP) and doxorubicin (DOX) to breast cancer cells using liposomal nanocarriers.
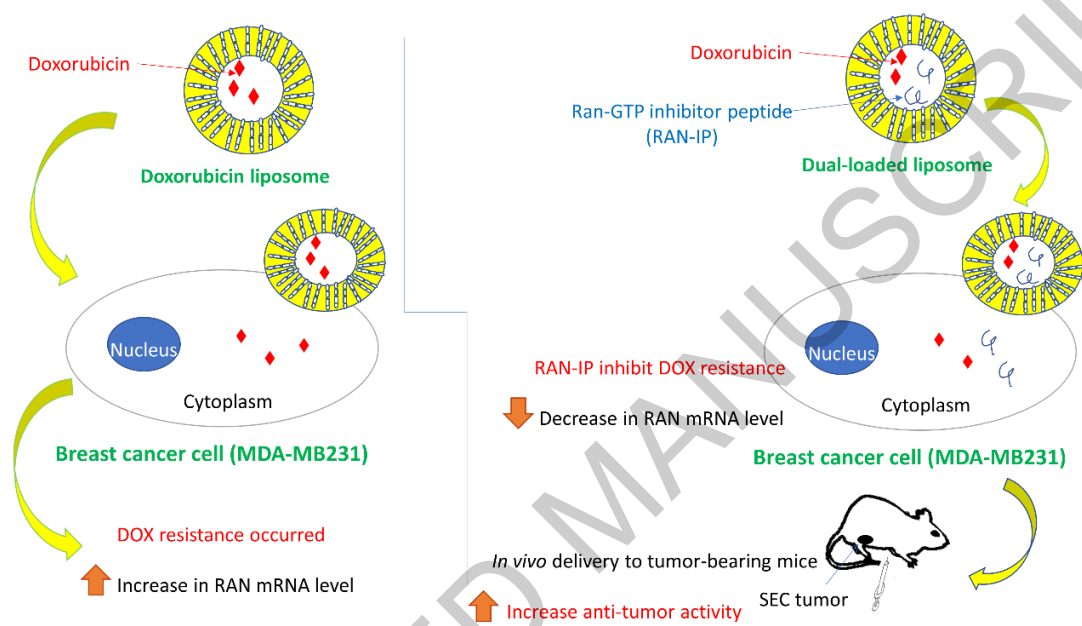
Research design: A liposomal delivery system, co-encapsulating DOX, and RAN-IP, was prepared using a thin-film rehydration technique. Dual-loaded liposomes were optimized by systematic modification of formulation variables. Real-Time-Polymerase Chain Reaction was used to determine Ran-GTP mRNA expression. In vitro cell lines were used to evaluate the effect of loaded liposomes on the viability of breast and lung cancer cell lines. In vivo testing was performed on a murine Solid Ehrlich Carcinoma model.

Results: RAN-IP reversed the Ran-expression-mediated MDR by inhibiting the Ran DNA damage repair function. Co-administration of RAN-IP enhanced sensitivity of DOX in breast cancer cell lines. Finally, liposome-mediated co-delivery with RAN-IP improved the anti-tumor effect of DOX in tumor-bearing mice when compared to single therapy.

Conclusions: This study is the first to show the simultaneous delivery of RAN-IP and DOX using liposomes can be synergistic with DOX and lead to tumor regression in vitro and in vivo.

Keywords: Doxorubicin, Ran-inhibitory peptide, Drug delivery, Liposome, Formulation variables, Optimization, Breast cancer

Graphical abstract

Doxorubicin

Doxorubicin liposome

Nucleus

Cytoplasm

Breast cancer cell (MDA-MB231)

DOX resistance occurred

Increase in RAN mRNA level

Doxorubicin

Ran-GTP inhibitor peptide (RAN-IP)

Dual-loaded liposome

RAN-IP inhibit DOX resistance

Decrease in RAN mRNA level

Nucleus

Cytoplasm

Breast cancer cell (MDA-MB231)

In vivo delivery to tumor-bearing mice

SEC tumor

Increase anti-tumor activity

1. Introduction

Breast cancer is a genetic disease, characterized by gene mutation, rearrangement, and amplification [1]. High mortality rates in industrialized countries are well documented [2], along with the limitations and adverse effects associated with the various protocols used during treatment [3]. It is a heterogeneous disease with several subtypes based on the expression of three different receptors, namely the progesterone, estrogen, and human epidermal growth factor receptor 2 (HER-2/neu)[4]. Clinical options share much with conventional chemotherapeutic strategies, based on the administration of cytotoxic drugs as a first-line approach, as is often the case with other types of cancer [5]. However, these types of regimens frequently induce multidrug resistance (MDR), leading to significant limitations in clinical outcomes [6]. MDR can develop over multiple rounds of continual chemotherapy and via various molecular mechanisms, including the regulation and deregulation of drug influx [7], mutation of drug targets, activation of DNA repair mechanisms, and deregulation of apoptosis [8].

Doxorubicin (DOX) is considered an orthodox chemotherapeutic drug. It is frequently used to treat solid tumors, such as breast, lung, gastric, ovarian, and thyroid cancers. The clinical use of DOX is limited severely by the risk of progressive, dose-dependent cardiomyopathy, and irreversible congestive heart failure [9,10]. There are considerable efforts in the field of DOX research on maintaining drug efficacy while reducing toxicity. It is administered as a monotherapy or, more commonly, in combination with other drugs and is primarily used in breast cancer treatment[11]. Its cytotoxic effect arises from inhibition of DNA topoisomerase II [12]. Unfortunately, the results of several studies have linked poor prognosis during DOX treatment with increased MDR [13]. For example, it has been shown that cancer cells evade the apoptotic effect of P53 by transporting it to the cytoplasm using a CRM1-mediated export mechanism[14].

Achieving an effective anti-tumor effect requires an understanding of the MDR pathway, prompting the development of attenuation strategies based on some form of interruptive intervention. A decrease of MDR, combined with the simultaneous use of a potent chemotherapeutic agent, is a potentially advantageous therapeutic strategy [15]. One approach has focused on novel delivery methods, such as anthracycline nano-

delivery systems, reported circumventing MDR effectively, both *in vitro* and *in vivo*[16,17]. This approach augments the therapeutic effect, whilst minimizing the expected adverse effects of high drug dosing [18]. Liposomes are of particular interest, having been successfully employed for the delivery of DOX. They possess a unique bilayer vesicular structure, comprising an internal aqueous compartment entrapped by one or more concentric lipid bilayers to facilitate the encapsulation of both lipophilic and hydrophilic drugs[19]. Liposomes have a number is beneficial properties, when compared to other nanosystems [20,21]. These properties include improving drug solubility, stability, and delivery to specific target sites [21]. Their sub-cellular size and lipid structure allow for higher intracellular uptake, which improves drug bioavailability when compared to other particulate systems. Furthermore, they provide drug protection against degradation while sustaining its release[20]. The main reason for selecting liposome as a drug nanocarrier is its significant role in effective drug delivery to target sites while minimizing systemic toxicity. Liposomal formulations have been shown to be beneficial for stabilizing therapeutic biomolecules, overcoming obstacles of cellular and tissue uptake, and improving the drug biodistribution to target sites *in vivo*. Liposomes exhibited positive outcomes in preclinical studies, thus the clinical translation of liposome-based drug delivery platforms has improved incrementally[22].

Our group has a particular interest in the functions of Ras-related nuclear protein (Ran). It is a key component of the exportin transport system and exists in two nucleotide forms [16]. It is best known for its roles in directional nucleocytoplasmic transport, mitotic spindle fiber assembly, and post-mitotic nuclear envelope dynamics[23]. Ran overexpression induces cellular transformation, tumorigenesis, and metastasis, both *in vitro* and *in vivo*[24,25]. Cancer cells with mutations and abnormal expression in proto-oncogenes and suppressors correlate to the activation of the PI3K/Akt/mTORC1 and Ras/MEK/ERK pathways, which are the most frequently dysregulated signaling pathways in cancer[26]. These pathways are more susceptible to Ran knockdown than normal cells [27,28].

The cellular compartmentalization of the Ran GTP-GDP cycle is regulated by the Ran guanine nucleotide exchange factor (RCC1). Besides, Ran-GAP creates a Ran-GTP gradient, which controls the transport of macromolecules between the nucleus and

the cytoplasm [26]. RanGTP-regulated nuclear export and import pathways control the cell cycle rate and cellular responses to DNA damage. If the cellular RanGTP concentration reaches a threshold, RanGTP-regulated nuclear-cytoplasmic transport reactions approach rates that support normal DNA Damage Response (DDR) function and cell cycle transitions. Consequently, DNA damage in such cells is successfully repaired, followed by termination of DDR and re-entry into the cell cycle. If RanGTP levels fall below the required threshold or a required nuclear transport receptor pathway is defective, the mechanisms of DNA repair or cell cycle re-entry are delayed. This, in turn, triggers cell cycle arrest or possible cell death [29]. The relation between Ran gene and DOX is controlled by the role of RCC-1. It was reported that, RCC1 promotes doxorubicin resistance in colorectal carcinoma cells. Besides, overexpression of RCC1 prevented the onset of DNA damage–induced cell senescence in normal cells. In case of colonic carcinoma, RCC1 overexpression strongly increased cell survival following doxorubicin-induced DNA damage. RCC1 overexpression was sufficient to accelerate cell cycle and DNA damage repair after DOX treatment[30].

Our group has reported previously, for the first time, on a specific peptide segment (CAQPEGQVQFK), known as Ran-RCC1 inhibitory peptide (RAN-IP). Its structure is based on the Ran protein sequence and blocks the interaction between RanGDP and RCC1 in MDA-MB231 breast cancer cells and A549 lung cancer cells. This competitive inhibition of the binding of RCC1 to its specific binding pocket present in the RanGDP conformation prevents RanGTP formation[23,31]. Experimental disruption of the guanine nucleotide cycle by RAN-IP has been demonstrated using RAN-IP-loaded nanoparticles, which prevent the generation of RanGTP by disrupting nucleotide-binding with RCC1, resulting in a dominant inhibitory effect on RanGTP formation. This suppresses tumorigenesis and metastasis both *in vitro* and *in vivo* [23,31].

Herein, we report on a novel liposome-based co-delivery of DOX and RAN-IP as combination chemotherapy for the first time. Importantly, the delivery of liposomal payloads comprising combinations of cytotoxic and peptide drugs has been reported elsewhere, such as paclitaxel and sorafenib, for reversion of multidrug resistance in vitro in breast cancer cells[32]. However, the peptide-based payload is used primarily

for targeting purposes and decorates the peripheral aspects of the liposome, as demonstrated by the co-delivery of DOX and vincristine for the treatment of glioma[33], DOX and erlotinib for treatment of glioblastoma[34] and DOX for treatment of lung metastasis[35].

The first aim of this work was to study the formulation and optimization of the physicochemical properties of liposomes loaded with both peptide and DOX using different formulation variables. The second aim was to use simultaneous liposomal delivery of DOX and RAN-IP to confirm the effect of reducing or reversing the overexpression of Ran during exposure to DOX. *In vitro* cytotoxicity of these dual functionalized liposomes was tested on breast and lung cancer cell lines (MDA-MB231, MCF-7, and A549). Finally, the study aimed to confirm that the upregulation of Ran in DOX-treated cells, *in vitro*, is a key mechanism that counteracts antineoplastic effects. The anti-tumor activity of dual functionalized liposomes was evaluated in an *in vivo* Solid Ehrlich Carcinoma (SEC) breast cancer model.

2. Materials and methods

2.1. Materials

1,2-Dipalmitoyl-sn-glycerol-3-phosphate-rac-(1-glycerol) (DPPG, sodium salt) and 1,2-dioleoyl-sn-glycerol-3-phosphoethanolamine (DOPE, purity >99%) were purchased from Avanti Polar Lipids, Inc., (Alabaster, AL). Peptide (NT 3-12) (MW 1243 Da, purity ≥ 96%) was synthesized by GL-Biochem Ltd. (Shanghai, China). Doxorubicin hydrochloride (DOX), cholesterol, methanol, dichloromethane, and phosphate-buffered saline were obtained from Sigma-Aldrich Company Ltd. (Poole, UK). Dichloromethane, acetonitrile, and trifluoroacetic acid were of HPLC grade and other reagents were of analytical grade. Water used in the work was produced to Type 1 standard (Milli-Q®, resistance of 18.2 MΩ cm at 25 °C, conductivity is   10 µS/cm, ion-free water at the sub-ppb level, total organic carbon is   30 µg/ml, and pH of 6.99).

2.2. Preparation of drug-loaded liposomes

Liposomes were prepared using a modified, thin-film rehydration method [36]. Phospholipids and cholesterol (DPPG: DOPE: cholesterol) of (4:4:2 molar ratio) were

dissolved in dichloromethane and methanol (3:1 v/v) in round bottom glassware. The organic solvent was evaporated at 40 °C using rotary evaporation. The resultant thin film was maintained under vacuum for 6 hours to ensure removal of residual solvents. The thin film was hydrated in a solution of NT 3-12 peptide in PBS for 1 hour at 60 °C using a bath sonication (150 W). The sample was frozen at -20 °C and then a freeze-thaw cycle repeated four times using bath sonication without addition of cryoprotectant. The sample was centrifuged at 22,000 g for 30 minutes at 4 °C for purification and removal of the non-encapsulated drug. DOX-loaded liposomes were prepared using this method, differing only in the rehydration step, where a PBS solution containing dissolved DOX was used. Dual-loaded liposomes containing both peptide and DOX were prepared using an identical procedure, but with a PBS solution containing dissolved NT 3-12 peptide and DOX for rehydration of the lipid film. Process variables, such as the pH of the dispersion medium, peptide loading and addition of DOX, are listed in (Table 1), together with the identifying code used to label each liposome formulation.

2.3. Characterisation of drug-loaded liposomes

Average size and population spread (polydispersity index) of liposome preparations were determined using dynamic light scattering (Nanosizer ZS, Malvern Instruments, UK). The particle size and distribution were measured after each freeze-Thaw cycle during preparation and after each week for one month during storage for measuring *in vitro* stability. Liposomal charge (Zeta potential) was determined using laser Doppler anemometry after a 5-fold dilution in distilled water (Nanosizer ZS, Malvern Instruments, UK). All measurements were performed in triplicate. Liposomal surface morphology was studied using transmission electron microscopy (JOEL JEM 2000 EX200) operating at an accelerating voltage of 80 kV. Samples were prepared by placing a suspension on a Formvar-coated grid and coating with a carbon layer (20 nm) under vacuum before scanning.

2.4. Determination of drug encapsulation efficiency

Peptide content was determined by an indirect procedure based on the determination of uncoated free peptide in the supernatant using HPLC [23,31]. Briefly, reversed-phase chromatography (Phenomenex- Luna® C18-5 column mm, 5 µm) with a flow rate of 1.0 ml per min, and UV detection (254 nm) was used. A mobile phase elution gradient was used, comprising two solvent mixtures (solvent A: 0.1% TFA in acetonitrile; solvent B: 0.1% TFA in water). Peptide encapsulation inside the liposome was calculated from the difference between the initial amount of peptide added and the free peptide remaining in the supernatant after liposome fabrication. DOX was detected using HPLC performed under conditions described elsewhere [37]. Chromatographic separation was accomplished with a mobile phase consisting of acetonitrile: water at a ratio of 30:70 (pH 3.0), and the drug was detected at 233 nm using a UV detector at a flow rate of 1.0 ml per min and ambient temperature. Each sample was assayed in triplicate and loading of both peptide and DOX reported as a percentage encapsulation efficiency (%E.E). Physicochemical characterizations of peptide-loaded, DOX-loaded and dual-loaded liposomes were represented in (Table 2).

2.5 In vitro release studies

A sample of peptide-loaded liposome formulation containing predetermined amounts of peptide and DOX was placed into a dialysis bag (10 kDa molecular weight cut off). The membrane was dialyzed against receptor media (50 ml PBS, pH 7.4). The release was studied at 37 °C at 100 rpm. At predetermined time interval points, a sample was removed (1.0 ml) replaced by an equal volume of fresh media to maintain sink conditions. Drug concentrations were assessed using HPLC, as described previously.

2.6. Cell culture

Breast cancer cell lines (MCF-7 and MDA-MB-231) and non-small cell lung carcinoma cells (A549) were obtained from the Cell Culture Department, VACSERA (Cairo, Egypt). Cells were routinely grown in T75 canted-neck tissue culture flasks. Cells were cultured in Dulbecco's Modified Eagle's Medium (DMEM) medium (Invitrogen/ Life Technologies, Grand Island, NY) supplemented with FBS (10% v/v), 10µg ml^{-1} of insulin and 1%

penicillin-streptomycin. The medium renewal was carried out every three days at 80% confluence. Cell cultures were incubated at 5% CO_2 and 37 °C.

2.7. In vitro cell viability assay

A cell viability assay was performed using an *in vitro* toxicology assay kit (MTT, 7H258, Sigma, Saint Louise, Missouri, USA) [38,39]. MCF-7, MDA-MB-231, and A549 cells (1.2-1.8 x10^4 cells/well in 100 µl media) were seeded in 96-well plates for 24 hours before treatment. The following day, all cells were treated with 100 µl of each of the following formulations: blank liposome, free peptide (1 µM), free DOX (1 µM), peptide-loaded liposome (1 µM), DOX-loaded liposome (1 µM), combination of both peptide-loaded liposome (1 µM) and DOX-loaded liposome (1 µM), dual-loaded liposome at three different concentrations (0.25, 0.5 and 1 µM). All treatments were suspended in transfection Optimem$^®$ media. Untreated MCF-7, MDA-MB-231, and A549 cells were used as controls.

Cell viability following each treatment was determined after 24, 48, and 72 hours. Treated cells were washed in PBS (100 µl) and 100 µl of reconstituted MTT (M-5655) dye solution in complete media was added to each well. The plates were incubated at 37 °C and 5% CO_2 for an additional 3 hours. The supernatant was discarded, solubilizing solution added (M-8910, 100 µl) and gently mixed in to dissolve the precipitate. The color intensity was measured at 570 nm and the background absorption measured at 690 nm in a microplate reader (Fluostar Omega, BMG Lab Tech GMBH, Germany). The anti-proliferative effect of different doses of free drugs and liposomal treatments was calculated as a percentage of cell growth concerning control cells. The absorbance of the untreated cells was set at 100%. The dose-effect curves were plotted for each treatment to measure the drug concentration that caused 50% growth inhibition (IC_{50})[40,41]. All experiments were performed in triplicate.

2.8. Real-time polymerase chain reaction

RNA was extracted using selective binding to silica-based membranes (RNeasy® Mini Kit, Qiagen Ltd., Manchester, UK), and reverse transcription was performed using SuperScript^{TM} III first-strand synthesis system (Invitrogen Ltd.) according to the

instructions supplied by the manufacturer. Real-time PCR (Applied Biosystem, Foster City, CA) was performed using an SYBR® Green assay for RanGTP and a forward primer 5' CCATCTTTCCAGCCTCAGTC 3' and reverse primer 5' CCAAGGAAGGCGTCTAAGGC 3'.

2.9. In vivo study

2.9.1. Animals

The *In vivo* study was performed on 60 female BALB/C mice, aged 7–8 weeks, and weighing 20 ± 2 g. They were housed in stainless steel mesh cages in ten groups of six. Mice were kept under standard conditions of light, relative humidity, and temperature, for ten days before the experiment. Animals had free access to standard laboratory food and water throughout the study. All procedures were performed according to a protocol approved by the Faculty of Pharmacy, Tanta University, and designed by the Animal Care and Use Committee.

2.9.2. Development of tumor model

The induction of a solid Ehrlich carcinoma tumor was performed as previously described [23,42]. Ehrlich ascites tumor (EAT) cells, supplied from the National Institute of Cancer, Egypt, were collected from the ascites fluid of female mice harboring 8–10-day old ascites tumor. Approximately, 2×10^6 viable EAT cells were suspended in PBS and injected subcutaneously into the back of BALB/C female mice. Growth was assessed daily until the tumor volume reached 100 mm^3. Volume was calculated by measuring both perpendicular diameters of the tumor using a digital caliper and applying the following equation [43].

$$\text{tumour volume } (\text{mm}^3) = 0.52.\,\text{length}.\,\text{width}^2$$

2.9.3. In vivo antitumor efficacy

To assess the *in vivo* antitumor efficacy of liposome formulations, animals were randomly separated into ten groups (six mice per each group). The study design of the *in vivo* experiment and treatment protocols are shown in (Table 3). The tumor-bearing mice were subdivided into groups, with each receiving an intraperitoneally administered

dose every three days for 16. At the end of the experiment, animals were sacrificed by cervical dislocation. The excised tumors were washed in cold saline, then weighed to determine the final tumor weight.

2.10. Biochemical assays

Lipid peroxide content in the heart tissue of treated animals was determined by measuring MDA (Biodiagnostic Ltd., Giza, Egypt). The method used colorimetric detection of the colored product formed following the reaction between thiobarbituric acid and the MDA content in heart tissue samples [44]. The assay procedures were conducted according to the protocol supplied by the manufacturer.

Serum lactate dehydrogenase (LDH) was measured by using a LDH kit (SPINREACT, Spain), following a method previously described [45]. Creatinine kinase (CK-MB) activity was measured using a propriety assay (Egyptian Company for Biotechnology, Cairo, Egypt) according to methods described elsewhere [46]. All serum samples were collected immediately before animal sacrifice.

2.11. Statistical analysis

Results for *in vitro* experiments were determined as mean ± SD and results from *in vivo* experiment were presented as mean ± SEM. The level of significance was evaluated statistically using a one-way ANOVA, followed by the post-hoc Tukey's test. $P < 0.05$ was considered to be statistically significant for both *in vitro* and *in vivo* experiments.

3. Results and discussion

Herein, we used thin film rehydration method followed by freeze-thaw cycle for preparation of drug-loaded liposomes. Thin film rehydration technique was adopted for encapsulation of hydrophilic drugs due to its simplicity, reproducibility, practicability, and its ability to yield small and uniform drug loaded liposomes after freeze-thaw cycles[47,48].

3.1. Effect of pH of the dispersion medium

The physicochemical characteristics of three different peptide-loaded liposome formulations (F1, F2, and F3) are shown in (Table. 2). NT 3-12 peptide was dissolved in aqueous dispersion media with each adjusted to one of the following pH values (PBS pH 7.4, phosphate buffer pH 6.8, and phosphate buffer pH 6) to investigate the effect of the pH value on the physicochemical properties of the peptide-loaded liposomes. Decreasing the pH of the aqueous dispersion medium resulted in a significant increase in liposomal size. The average size of (F1) rehydrated by phosphate buffer (pH 6) was found to be 139 ± 21 which was significantly bigger (p   0.01) compared to 81 ± 11nm in the case of (F3) prepared at higher pH of 7.4. Low pH values cause the protonation of the phospholipid heads and therefore hydrogen bond formation may occur resulting in bigger liposomal size meanwhile some phospholipid may exhibit electrostatic repulsion between protonated phospholipid heads. In the case of DPPG, protonation of phospholipid heads was more likely to occur compared to other lipids so that hydrogen bond formation between adjacent protonated heads predominate the electrostatic repulsion resulting in larger liposome size [49,50]. The change in pH value of the dispersion medium showed a slight change in zeta potential (p   0.05). This might be attributed to the poor electrostatic repulsion effect resulted from the change in pH values.

Increasing pH value from 6 to neutral 7.4 resulted in a significant increase in peptide encapsulation efficiency. The average % E.E of (F1) prepared at a low pH value of 6 was found to be 52.13 ± 7.96 which was significantly lower than % E.E of 93.15% ± 6.1% in case (F3) prepared at higher pH of 7.4 (p   0.001). This can be explained by the hydrogen bond formation between neighbouring protonated heads of DPPG at lower

pH which decreases their hydrophilicity. This subsequently decreases the hydration of the lipid film by the aqueous drug-containing medium leading to a lower encapsulation efficiency. On the other hand, smaller liposome size resulted at pH 7.4 exhibited higher surface area available for lipid hydration with aqueous drug-medium resulting in a higher percentage of peptide encapsulation[49,50].

In vitro release profiles of different peptide-loaded liposomes (F1, F2, and F3) showed a significant decrease ($p < 0.05$) in initial burst release phase in the case of F3 compared to both F1 and F2 (Fig. 1A). Burst release after 24 h was 59.17% ± 8.36%, 53.13% ± 5.11%, and 44.66% ± 5.7% in case of F1, F2 and F3, respectively. This lower initial burst is preferable especially in case of in vivo administration of nano-drug delivery system reducing the risk of premature drug release before reaching the targeted site of action [31].

3.2. Effect of peptide loading

The physicochemical properties of the three peptide-loaded liposome formulations (F3, F6, and F9) were recorded in (Table 2). Three peptide loadings levels (3%, 5%, and 7% w/w) were used in this study while maintaining the lipid composition and concentration. Increasing peptide loading resulted in a significant increase in the liposomal size (p 0.05). liposome size increased from 81 ± 11 nm in the case of 3% w/w peptide loading (F3) to 128 ± 14 nm in the case of 7% w/w peptide loading (F9) (p 0.01). Increasing the peptide loading might have resulted in the separation of the concentric lipid bilayers encapsulating the aqueous drug core due to the high molecular weight of the dissolved peptide leading to the increasing of liposomal surface area and therefore size [51]. The lower level of peptide loading of 3% w/w (F3) showed a significant decrease in polydispersity compared to a higher peptide loading level of (F7) (p 0.05). Peptide loading showed no significant effect on the zeta potential of the liposomes ($p > 0.05$).

On the other hand, drug loading had a significant impact on the encapsulation efficiency of peptide inside liposomes. The increase in peptide loading resulted in a significant decrease in encapsulation efficiency ($p < 0.05$). Results showed that encapsulation efficiency observed for F7 was significantly decreased to 64.7% ± 2.1% compared to

93.15% ± 6.1% for (F3) (p 0.01). This might be attributed to the inability of phospholipid structure to entrap this high mount of peptide inside its aqueous drug layers [52].

In vitro release profiles and the initial burst release were closely related to the degree of peptide loading (Fig.1B). The burst release of F3 with peptide loading of 3% w/w was significantly lower than those of (F9) with 7% peptide loading (p < 0.01). Initial bursts of 44.7% ± 5.7%, 56.2% ± 6.1% and 65.9% ± 4.2% were observed from F3, F6 and F9, respectively. High peptide loading in the dispersion medium enhanced the saturation of liposomal structure with peptide creating a relatively higher concentration gradient driving a higher rate of diffusion of peptide towards the external aqueous release phase increasing burst and total *in vitro* release [53].

According to the previous results, it was clear that F3 was found to be the optimum peptide-loaded liposome formulation as it has the lowest size, highest zeta potential, highest encapsulation efficiency, and lowest initial burst release. Therefore, the same formulation conditions adopted for preparing (F3) were used for co-encapsulation of peptide and DOX in the same liposome to prepare (double-loaded liposome).

3.3. Effect of adding DOX

In this part of the study, DOX was dissolved along with the NT 3-12 peptide in the same aqueous dispersion medium of (PBS, pH 7.4) to investigate the effect of adding DOX on the physicochemical characterization of different peptide-loaded liposomes (Table 2). The addition of DOX to peptide-loaded liposomes as in the case of (F11) demonstrated no significant increase of the mean liposome size compared to (F3) prepared without Dox (p > 0.05). A significant decrease in zeta potential was observed (p < 0.05). A slight decrease in peptide % E.E was observed. On the other hand, the % E.E of doxorubicin was 80.6%. Nonetheless, a significant increase in the initial burst release of the peptide was also observed (p < 0.05) (Fig. 1.C). This might be attributed to the displacement effect of the loaded DOX on the loaded peptide resulting in lower encapsulation efficiency and higher initial release [54]. Approximately, 58% of peptide was released after 24 h which accounted for the drug adsorbed on the surface of the liposomes.

However, 99 % of peptide was released after 72 h, due to the drug encapsulated inside the inner aqueous core of the dual-loaded liposomes. These results indicated the presence of drug in both adsorbed form and encapsulated. On the other hand, DOX showed a different release profile with a significantly lower initial burst release ($p < 0.01$) of 35.7% compared to 58.6 % of peptide released from F11. Faster DOX release was observed after the first 24 hours with almost 97.3% released after 48 hours. The fast release of DOX after 24 hours may be due to high diffusion of the encapsulated drug towards the dissolution media depending on its small molecular weight compared to the high molecular weight of the encapsulated peptide. In addition, membrane fluidity of the prepared liposomes might contribute to the high DOX release. Incorporation of DOPE with low phase transition temperature Tc of -16 increased the fluidity of the liposomal membrane which facilitated doxorubicin release[55]. *In vitro* release, results showed that peptide and Dox can be released efficiently from the dual loaded liposomal carrier.

Based on the above results, F11 was used for further *in vitro* and *in vivo* experiments due to its superior physiochemical properties compared to other formulations as demonstrated by its optimum mean size, zeta potential, encapsulation efficiency and *in vitro* release of both drugs.

3.4. Transmission electron microscopy

To visualize the surface morphology of the double-loaded liposome (F11), TEM was used to assess the liposome morphology. TEM images revealed a smooth spherical shape of homogenous size, with no evidence of liposome adhesion or aggregation (Fig. 2.A). The average size obtained using TEM showed no significant differences when compared to similar data captured using light scattering.

To ensure the stability of this formulation (F11), a sample was stored in a fridge at 4°C for 4 weeks and its particle size was measured periodically. The results show that the particle size showed a non-significant increase after 3 weeks compared to freshly prepared liposomes ($p > 0.05$). A significant increase in liposomal size (p 0.05) was noticed on day 28 after preparation (Fig 2.B). The % E.E of both peptide and

doxorubicin showed a non-significant change after 5 days of preparations (p   0.05). Therefore, freshly prepared samples were used continuously for *in vivo* study.

3.5. In vitro cell viability assay

The cytotoxic action of different liposomal treatments on the MDA-MB 231, MCF-7, and A549 cell lines were evaluated by MTT assay 24, 48, and 72 hours after treatment (Fig. 3). MDA-MB 231 and MCF-7 breast cancer cell lines were used efficiently as a model for studying doxorubicin resistance[56]. Besides, A549 cell line is one of resistant lung cell lines against doxorubicin treatment[57]. The results show that the blank liposome and free peptide had no cytotoxicity on breast and lung cancer cells. Treatment with peptide-loaded liposome (1μM) showed a significant reduction in cell viability compared to the control and free peptide (p < 0.05). This confirms the subcellular delivery of peptide inside the cancer cell where it can achieve its action on Ran inactivation as we previously reported [23,31]. On the other hand, treatment with free DOX and DOX-loaded liposomes showed a significant reduction in cell viability compared to control cells (p < 0.05). However, treatment with DOX-loaded liposome showed more cytotoxic action compared to the free drug (p < 0.01). These results were in good agreement with other previously reported [58]. The dose-effect curves were plotted to measure the liposomal drug concentration that caused 50% growth inhibition (IC_{50}). Double-loaded liposome (F11) showed a dose-dependent cytotoxic action in all cell lines as cell viability decreased with increasing the dose from 0.25 to 1 μM. Treatment of MDA-MB 231 breast cancer cells with double-loaded liposome reduced cell viability in a dose-dependent manner while maintaining its cytotoxic action up to three days after treatment due to sustained cytotoxic action (Fig. 3.A). After 24 hours of treatment, the mean IC_{50} value of double-loaded liposome (F11) in MDA-MB 231 cells was 0.304 ± 0.08 μM. This IC_{50} value is significantly lower than previously calculated IC_{50} of our peptide-loaded polymeric nanoparticles which was estimated to be 3.6 μM (p < 0.001) [31]. This might be due to the co-delivery of DOX and peptide together in the same liposome as well as to the nature of the liposomes as a superior drug delivery vehicle. Higher cytotoxic action was observed after the treatment of MCF-7 breast cancer cells with double-loaded liposomes. A similar dose-dependent effect was demonstrated in the case of

MCF-7 cells. The mean IC_{50} value of (F11) in the case of MCF-7 cells was 0.112 ± 0.05 µM, which was significantly lower than IC_{50} of the same treatment in MDA-MB 231 cells calculated after 24 hours ($p < 0.01$) (Fig. 3.B). Treatment of lung cancer cells with (F11) showed a similar dose-dependent cytotoxic action up for three days after treatment (Fig. 3.C). The mean IC_{50} value for (F11) in A549 cells was 0.416 ± 0.12 µM, compared to similar IC_{50} values for MDA-MB 231 and MCF-7, respectively ($p < 0.05$). Cell viability results showed a non-significant decrease in cell viability after 72 hours compared to 48 hours (p 0.05) especially in lung cancer cells. This might be attributed to cell saturation with both drugs. Besides, *in vitro* release results showed a non-significant difference between the amount of peptide and doxorubicin released after 48 and 72 hours from the double-loaded liposomes.

Based on these results, double-loaded liposome (F11) achieved a significant reduction in cell viability ($p < 0.001$) compared to free peptide, peptide-loaded liposome, free DOX, and DOX-loaded liposome. Besides, F11 showed a significant cytotoxic action compared to the combination of both peptide-loaded and DOX-loaded liposomes. This might be attributed to the synergistic anti-cancer effect resulted from the co-delivery of peptide and DOX in one liposomal form. Double-loaded liposome achieved successful peptide and DOX delivery to the subcellular site of action meanwhile preserving their anti-cancer activity after formulation.

3.6. Quantitative Real-time PCR

To explain the results of the cell viability study, qPCR was carried out to investigate the effect of Dox on mRNA ran expression. The results were analysed as mean ± SD by use of analysis of variance (ANOVA) with Dunnett's multiple comparisons test using GraphPad prism 8.1.2. (Fig. 4.A) shows RAN mRNA expression level in MDA-MB-231 cell-line following treatment with Dox 1µM at three-time points (6,12 and 24h). RAN mRNA expression was downregulated after 6 and 12 hours treated by 1µM Dox by 40% and 20%, respectively compared to control empty liposome treated cells. This could be due to a decrease in cell viability.

At 24 hours, however, the level of Ran mRNA expression was significantly increased by 100% compared to the control and by 200% compared to the 6hrs level. Following the treatment of MDA-MB231 cell by Dox at 1.3 μM, Ran mRNA expression was decreased by 20% at 6 hours compared to empty liposome treated cells but increased at 12 and 24 hrs to 110% and 200%, respectively compared to the cells treated by empty liposome. The addition of the liposomal RAN-GTP blockade peptide counteracted the overexpression in RAN mRNA due to the treatment with DOX (Fig. 4.B).

Ran overexpression may help cancer cells resistance to DOX. It has been shown that Ran has an important role in DNA damage repair, thus introducing a RAN inhibitor will neutralize this effect and synergize the effect of DNA damage caused by DOX and, thus, increase cell apoptosis. *In vitro* results showed that DOX inhibited RAN expression in cells then after 24 hours RAN expression was upregulated hence cells are resisting the cytotoxic effect of DOX. The after treating with RAN-IP, the RAN expression was downregulated again and re-sensitize the cells to DOX.

3.7. In vivo studies

3.7.1. In vivo antitumor efficacy

This study was performed using the SEC model to investigate the anti-cancer activity of prepared nano-drug delivery systems on breast cancer-induced in mice. The SEC model was carefully selected for this study due to the following reasons. Firstly, SEC is a well-established murine mammary adenocarcinoma model in tumor biology. This model has largely been used for study of tumor pathogenesis and development of anti-tumorigenic agents[59]. Secondly, the Ehrlich model is used extensively in studying the MDR of different chemotherapeutics such as daunorubicin, Mitoxantrone, etoposide[60-62]. Finally, Doxorubicin has been shown to induce expression of P-gp after only 24 h of contact with sensitive Ehrlich cells[61,63,64]. Therefore, this model can develop MDR to doxorubicin in a very short time of only 24 hours[63], meanwhile, the duration of our *in vivo* study was 16 days. The antitumor activity of peptide-loaded liposome, Dox-loaded liposome, and double-loaded liposome (Table 3) was demonstrated in (Fig. 5).

Intraperitoneal administration (IP) of liposomal drug delivery systems was selected due to its numerous advantages. Previous studies showed that, intraperitoneal administration of siRNA-loaded liposomes was as efficient as intravenous administration for treatment of ovarian cancer. Liposomes injected IP were distributed by diffusion into intraperitoneal cavity through the vasculature, rather than direct diffusion to reach the tumor site from the peritoneal cavity[65]. IP administration of doxorubicin-loaded liposome was the best choice for treatment of SEC model *in vivo* due to its significant effect on prolongation of survival time of treated animals due to its leaky properties and high peritoneal dissemination of these liposomes[66]. After 16 days of treatment, the control and blank liposome-treated groups showed an increase in tumor volume by 281.93% and 312.25%, respectively. Animals treated with free peptide (10 mg kg^{-1}) showed no anti-tumor activity as tumor volumes increased by 354.24%. Mice treated by peptide-loaded liposome (10 mg kg^{-1}), free DOX (5 mg kg^{-1}) and DOX liposome (5 mg kg^{-1}) exhibited a significant tumour growth inhibition of 55.4%, 50.22% and 65.91% respectively ($p < 0.001$) (Fig. 6). The animal group treated with the combination of peptide liposome (10 mg kg^{-1}) and DOX liposome (5 mg kg^{-1}) demonstrated a 78.61% reduction in tumor volume that was significantly more effective than the use of each single-drug loaded liposome ($p < 0.001$). Treatment with double-loaded liposomes showed the highest % of tumor growth inhibition of 85.91%, 95.55%, and 97.77% in cases of 1X, 2X, and 3X, respectively. The most favourable antitumor activity was observed in animals treated with double-loaded liposomes (2X and 3X). These results confirm the superiority of synergistically combined therapy of NT 3-12 peptide and DOX. This is the first time to report the anticancer activity of the combination of NT 3-12 peptide and DOX by co-delivery of both drugs in a liposome-based drug delivery system.

At the end of the treatment, all animals were sacrificed. A photograph of excised tumors for each animal group was shown in (Fig. 7). The difference in tumor weights between control and treated animals was exhibited in (Fig. 8). The average tumor weight in the control group after treatment was 3.95 ± 0.46 g. Animals treated with double-loaded liposomes showed a reduction in average tumor weight of 91.13 %, 97.46%, and 99.49% in cases of 1X, 2X, and 3X, respectively ($p < 0.001$).

3.7.2. In vivo safety

There were no signs of decreased activity or abnormal behaviour, which indicates no toxicity caused by all treatments. Most animals appeared healthy and no substantial body weight loss was observed (Fig. 9). However, animals treated with free DOX and DOX-loaded liposomes showed a significant body weight loss compared to the control animal ($p < 0.05$). Biochemical assays were done to investigate the cardiotoxicity of DOX-loaded liposome in vivo. Three different biochemical parameters of cardiac MDA, LDH, and CK-MB levels were investigated, and results were presented in (Table 4). Tumor-bearing animals served as a control group showed a non-significant (P 0.05) increase in cardiac MDA compared to normal animals. Mice treated with free DOX and DOX-loaded liposome showed a significant increase in cardiac MDA levels compared to control animals and animals treated with peptide-loaded liposome. However, DOX-loaded liposome showed a non-significant decrease in MDA level compared to free DOX. This was due to the cardiotoxic effect of DOX *in vivo*. Besides, treatment with free DOX and DOX-loaded liposomes resulted in a significant increase in LDH and CK-MB activity levels. However, DOX-loaded liposome showed a significant decrease in CK-MB level compared to free DOX treated animals ($p < 0.05$). Fortunately, double-loaded liposomes showed a non-significant increase in cardiac MDA, LDH, and CK-MB levels compared to control animals which can confirm its safety for *in vivo* use.

4. Conclusions

Peptide-loaded liposomes were prepared using a thin film rehydration technique comprising several peptides and DOX loading levels, and variable pH of the dispersion media. An optimum double-loaded liposome was selected, which had the highest peptide loading of 85%, the lowest particle size of 80 nm, whilst sustaining the peptide and Dox release for 3 days. *In vitro* cell viability studies of peptide-loaded liposomes showed superior cytotoxic action compared to free peptide and free Dox. The highest reduction in cell viability was observed in case of MCF-7 due to the lowest IC_{50} of 0.112 ± 0.05 compared to 0.304 ± 0.08 and 0.416 ± 0.12 µM for MDA-MB-231 and A549, respectively after treatment with double-loaded liposome. Dox treatment was shown to cause a significant increase in RanGTP mRNA level, and this increase was successfully reversed when RAN-IP was included in the treatment. The *in vivo* results confirmed the enhanced anti-cancer activity of double-loaded liposome by achieving 85.91%, 95.55%, and 97.77% tumor growth inhibition after treatment with different doses of 1X, 2X and 3X of the double-loaded liposome. Toxicity examinations showed that a combined-drug delivery system was found to be safer to liver and kidney tissues when compared to the free DOX. The emergence of a novel drug delivery system is of high clinical importance because it will improve the therapeutic response by providing a synergistic anti-tumor effect both *in vitro* and *in vivo* along with causing minimal side effects compared to classic dosage forms of the same drugs.

Author contributions

Conceptualization and design: Y Haggag, B Abu Ras, M Isreb, M El-Tanani; Analysis and interpretations of data, Y Haggag, Y El-Tanani, M Tambuwala, P McCarron, M El-Tanani; Writing and drafting the paper: Y Haggag, Y El-Tananai, B Abu Ras, M Isreb, M El-Tanani; All authors have read and agreed to the published version of the manuscript.

Funding

This paper was not funded.

Declaration of interest

The authors have no other relevant affiliations or financial involvement with any organization or entity with a financial interest in or financial conflict with the subject matter or materials discussed in the manuscript apart from those disclosed.

Reviewer disclosures

Peer reviewers on this manuscript have no relevant financial or other relationships to disclose.

References

1.	Merlo LM, Pepper JW, Reid BJ, et al. Cancer as an evolutionary and ecological process. Nature reviews Cancer. 2006 Dec;6(12):924-35.

2.	Siegel RL, Miller KD, Jemal A. Cancer statistics, 2019. CA: a cancer journal for clinicians. 2019 Jan;69(1):7-34.

3.	Atkins MB, Tannir NM. Current and emerging therapies for first-line treatment of metastatic clear cell renal cell carcinoma. Cancer treatment reviews. 2018 Nov;70:127-137.

4.	Haffty BG, Yang Q, Reiss M, et al. Locoregional relapse and distant metastasis in conservatively managed triple negative early-stage breast cancer. Journal of clinical oncology : official journal of the American Society of Clinical Oncology. 2006 Dec 20;24(36):5652-7.

5.	Dawar S, Singh N, Kanwar RK, et al. Multifunctional and multitargeted nanoparticles for drug delivery to overcome barriers of drug resistance in human cancers. Drug Discov Today. 2013 Dec;18(23-24):1292-300.

6.	Coley HM. Mechanisms and strategies to overcome chemotherapy resistance in metastatic breast cancer. Cancer Treat Rev. 2008 Jun;34(4):378-90.

7.	Szakacs G, Hall MD, Gottesman MM, et al. Targeting the Achilles heel of multidrug-resistant cancer by exploiting the fitness cost of resistance. Chem Rev. 2014 Jun 11;114(11):5753-74.

8.	Markman JL, Rekechenetskiy A, Holler E, et al. Nanomedicine therapeutic approaches to overcome cancer drug resistance. Advanced drug delivery reviews. 2013 Nov;65(13-14):1866-79.

9.	Minotti G, Menna P, Salvatorelli E, et al. Anthracyclines: molecular advances and pharmacologic developments in antitumor activity and cardiotoxicity. Pharmacol Rev. 2004 Jun;56(2):185-229.

10.	Minotti G, Recalcati S, Menna P, et al. Doxorubicin cardiotoxicity and the control of iron metabolism: quinone-dependent and independent mechanisms. Methods Enzymol. 2004;378:340-61.

11. Capelôa T, Benyahia Z, Zampieri LX, et al. Metabolic and non-metabolic pathways that control cancer resistance to anthracyclines. Seminars in cell & developmental biology. 2020 Feb;98:181-191.

12. Aas T, Børresen A-L, Geisler S, et al. Specific P53 mutations are associated with de novo resistance to doxorubicin in breast cancer patients. Nature Medicine. 1996 1996/07/01;2(7):811-814.

13. Loi S, Pommey S, Haibe-Kains B, et al. CD73 promotes anthracycline resistance and poor prognosis in triple negative breast cancer. Proceedings of the National Academy of Sciences of the United States of America. 2013 Jul 2;110(27):11091-6.

14. Shen J, He Q, Gao Y, et al. Mesoporous silica nanoparticles loading doxorubicin reverse multidrug resistance: performance and mechanism. Nanoscale. 2011 Oct 5;3(10):4314-22.

15. Iyer AK, Singh A, Ganta S, et al. Role of integrated cancer nanomedicine in overcoming drug resistance. Advanced drug delivery reviews. 2013 Nov;65(13-14):1784-802.

16. Turner JG, Dawson J, Sullivan DM. Nuclear export of proteins and drug resistance in cancer. Biochemical Pharmacology. 2012;83(8):1021-1032.

17. Nielsen D, Maare C, Poulsen F, et al. The relationship between resistance, P-glycoprotein content, and steady state accumulation in five series of Ehrlich ascites tumor cell lines selected for resistance to daunorubicin. Cell Pharmacol. 1994;1:127-135.

18. Zununi Vahed S, Salehi R, Davaran S, et al. Liposome-based drug co-delivery systems in cancer cells. Materials Science and Engineering: C. 2017 2017/02/01/;71:1327-1341.

19. Torchilin V, Weissig V. Liposomes: a practical approach. Oxford University Press; 2003. (264).

20. Bulbake U, Doppalapudi S, Kommineni N, et al. Liposomal Formulations in Clinical Use: An Updated Review. Pharmaceutics. 2017;9(2):12.

21. Chen X, Wang X, Wang Y, et al. Improved tumor-targeting drug delivery and therapeutic efficacy by cationic liposome modified with truncated bFGF peptide.

Journal of controlled release : official journal of the Controlled Release Society. 2010 Jul 1;145(1):17-25.

22.   Sercombe L, Veerati T, Moheimani F, et al. Advances and Challenges of Liposome Assisted Drug Delivery. Frontiers in pharmacology. 2015;6:286-286.

23.   Haggag YA, Matchett KB, Falconer RA, et al. Novel Ran-RCC1 Inhibitory Peptide-Loaded Nanoparticles Have Anti-Cancer Efficacy In Vitro and In Vivo. Cancers. 2019 Feb 14;11(2).

24.   Kurisetty VV, Johnston PG, Johnston N, et al. RAN GTPase is an effector of the invasive/metastatic phenotype induced by osteopontin. Oncogene. 2008 Dec 04;27(57):7139-49.

25.   Yuen HF, Chan KK, Grills C, et al. Ran is a potential therapeutic target for cancer cells with molecular changes associated with activation of the PI3K/Akt/mTORC1 and Ras/MEK/ERK pathways. Clin Cancer Res. 2012 Jan 15;18(2):380-91.

26.   Clarke PR, Zhang C. Spatial and temporal coordination of mitosis by Ran GTPase. Nat Rev Mol Cell Biol. 2008 Jun;9(6):464-77.

27.   Yuen H-F, Chan K-K, Platt-Higgins A, et al. Ran GTPase promotes cancer progression via Met receptormediated downstream signaling. 2016. (2016).

28.   Yuen HF, Gunasekharan VK, Chan KK, et al. RanGTPase: a candidate for Myc-mediated cancer progression. Journal of the National Cancer Institute. 2013 Apr 3;105(7):475-88.

29.   Cekan P, Hasegawa K, Pan Y, et al. RCC1-dependent activation of Ran accelerates cell cycle and DNA repair, inhibiting DNA damage-induced cell senescence. Mol Biol Cell. 2016 Apr 15;27(8):1346-57.

30.   Cekan P, Hasegawa K, Pan Y, et al. RCC1-dependent activation of Ran accelerates cell cycle and DNA repair, inhibiting DNA damage-induced cell senescence. Molecular biology of the cell. 2016;27(8):1346-1357.

31.   Haggag YA, Matchett KB, Dakir El H, et al. Nano-encapsulation of a novel anti-Ran-GTPase peptide for blockade of regulator of chromosome condensation 1 (RCC1) function in MDA-MB-231 breast cancer cells. International journal of pharmaceutics. 2017 Apr 15;521(1-2):40-53.

32.	Lei M, Ma G, Sha S, et al. Dual-functionalized liposome by co-delivery of paclitaxel with sorafenib for synergistic antitumor efficacy and reversion of multidrug resistance. Drug delivery. 2019;26(1):262-272.

33.	Zhang Y, Zhai M, Chen Z, et al. Dual-modified liposome codelivery of doxorubicin and vincristine improve targeting and therapeutic efficacy of glioma. Drug delivery. 2017 2017/01/01;24(1):1045-1055.

34.	Lakkadwala S, dos Santos Rodrigues B, Sun C, et al. Dual functionalized liposomes for efficient co-delivery of anti-cancer chemotherapeutics for the treatment of glioblastoma. Journal of Controlled Release. 2019 2019/08/10/;307:247-260.

35.	Ierano C, Portella L, Lusa S, et al. CXCR4-antagonist Peptide R-liposomes for combined therapy against lung metastasis. Nanoscale. 2016 Apr 14;8(14):7562-71.

36.	Roy B, Guha P, Bhattarai R, et al. Influence of Lipid Composition, pH, and Temperature on Physicochemical Properties of Liposomes with Curcumin as Model Drug. Journal of oleo science. 2016;65(5):399-411.

37.	Dharmalingam SR, Ramamurthy S, Chidambaram K, et al. A simple HPLC bioanalytical method for the determination of doxorubicin hydrochloride in rat plasma: application to pharmacokinetic studies. Tropical journal of pharmaceutical research. 2014;13(3):409-415.

38.	Haggag YA, Ibrahim RR, Hafiz AA. Design, Formulation and in vivo Evaluation of Novel Honokiol-Loaded PEGylated PLGA Nanocapsules for Treatment of Breast Cancer. International journal of nanomedicine. 2020;15:1625-1642.

39.	Haggag Y, Elshikh M, El-Tanani M, et al. Nanoencapsulation of sophorolipids in PEGylated poly(lactide-co-glycolide) as a novel approach to target colon carcinoma in the murine model. Drug Deliv Transl Res. 2020 Apr 1.

40.	Haggag Y, Elshikh M, El-Tanani M, et al. Nanoencapsulation of sophorolipids in PEGylated poly(lactide-co-glycolide) as a novel approach to target colon carcinoma in the murine model. Drug Delivery and Translational Research. 2020 2020/04/01.

41.   Yuen HF, Chan KK, Platt-Higgins A, et al. Ran GTPase promotes cancer progression via Met receptormediated downstream signaling. Oncotarget. 2016 Oct 03.

42.   Haggag YA, Osman MA, El-Gizawy SA, et al. Polymeric nano-encapsulation of 5-fluorouracil enhances anti-cancer activity and ameliorates side effects in solid Ehrlich Carcinoma-bearing mice. Biomedicine & Pharmacotherapy. 2018;105:215-224.

43.   Papadopoulos D, Kimler BF, Estes NC, et al. Growth delay effect of combined interstitial hyperthermia and brachytherapy in a rat solid tumor model. Anticancer research. 1989 Jan-Feb;9(1):45-7.

44.   Yoshioka T, Kawada K, Shimada T, et al. Lipid peroxidation in maternal and cord blood and protective mechanism against activated-oxygen toxicity in the blood. American journal of obstetrics and gynecology. 1979 Oct 1;135(3):372-6.

45.   Buhl SN, Jackson KY. Optimal conditions and comparison of lactate dehydrogenase catalysis of the lactate-to-pyruvate and pyruvate-to-lactate reactions in human serum at 25, 30, and 37 degrees C. Clinical chemistry. 1978 May;24(5):828-31.

46.   Rosalki SB. An improved procedure for serum creatine phosphokinase determination. The Journal of Laboratory and Clinical Medicine. 1967;69(4):696-705.

47.   Zhang H. Thin-Film Hydration Followed by Extrusion Method for Liposome Preparation. Methods in molecular biology (Clifton, NJ). 2017;1522:17-22.

48.   Ai X, Zhong L, Niu H, et al. Thin-film hydration preparation method and stability test of DOX-loaded disulfide-linked polyethylene glycol 5000-lysine-di-tocopherol succinate nanomicelles. Asian Journal of Pharmaceutical Sciences. 2014 2014/10/01/;9(5):244-250.

49.   Garidel P, Johann C, Mennicke L, et al. The mixing behavior of pseudobinary phosphatidylcholine-phosphatidylglycerol mixtures as a function of pH and chain length. European biophysics journal. 1997;26(6):447-459.

50. Sułkowski W, Pentak D, Nowak K, et al. The influence of temperature, cholesterol content and pH on liposome stability. Journal of Molecular Structure. 2005;744:737-747.

51. Brgles M, Jurasin D, Sikiric MD, et al. Entrapment of ovalbumin into liposomes--factors affecting entrapment efficiency, liposome size, and zeta potential. Journal of liposome research. 2008;18(3):235-48.

52. Chountoulesi M, Naziris N, Pippa N, et al. The significance of drug-to-lipid ratio to the development of optimized liposomal formulation. Journal of liposome research. 2018 Sep;28(3):249-258.

53. Johnston MJ, Edwards K, Karlsson G, et al. Influence of drug-to-lipid ratio on drug release properties and liposome integrity in liposomal doxorubicin formulations. Journal of liposome research. 2008;18(2):145-57.

54. Tefas LR, Sylvester B, Tomuta I, et al. Development of antiproliferative long-circulating liposomes co-encapsulating doxorubicin and curcumin, through the use of a quality-by-design approach. Drug design, development and therapy. 2017;11:1605.

55. Li J, Wang X, Zhang T, et al. A review on phospholipids and their main applications in drug delivery systems. Asian Journal of Pharmaceutical Sciences. 2015 2015/04/01/;10(2):81-98.

56. Marinello PC, Panis C, Silva TNX, et al. Metformin prevention of doxorubicin resistance in MCF-7 and MDA-MB-231 involves oxidative stress generation and modulation of cell adaptation genes. Scientific Reports. 2019 2019/04/10;9(1):5864.

57. Xu L, Li H, Wang Y, et al. Enhanced activity of doxorubicin in drug resistant A549 tumor cells by encapsulation of P-glycoprotein inhibitor in PLGA-based nanovectors. Oncol Lett. 2014;7(2):387-392.

58. Lao J, Madani J, Pu, et al. Liposomal Doxorubicin in the Treatment of Breast Cancer Patients: A Review. Journal of Drug Delivery. 2013;2013:12.

59. Mishra S, Tamta AK, Sarikhani M, et al. Subcutaneous Ehrlich Ascites Carcinoma mice model for studying cancer-induced cardiomyopathy. Scientific reports. 2018;8(1):5599-5599.

60. Nielsen D, Maare C, Eriksen J, et al. Characterisation of multidrug-resistant Ehrlich ascites tumour cells selected in vivo for resistance to etoposide. Biochemical pharmacology. 2000 Aug 1;60(3):353-61.

61. Nielsen D, Eriksen J, Maare C, et al. P-glycoprotein expression in Ehrlich ascites tumour cells after in vitro and in vivo selection with daunorubicin. British journal of cancer. 1998 Nov;78(9):1175-80.

62. Nielsen D, Eriksen J, Maare C, et al. Characterisation of non-P-glycoprotein multidrug-resistant Ehrlich ascites tumour cells selected for resistance to mitoxantrone. Biochemical pharmacology. 2000 Aug 1;60(3):363-70.

63. Volm M, Mattern J, Pommerenke E. Time course of MDR gene amplification during in vivo selection for doxorubicin-resistance and during reversal in murine leukemia L 1210. Anticancer research. 1991;11(2):579.

64. Chevillard S, Vielh P, Bastian G, et al. A single 24h contact time with adriamycin provokes the emergence of resistant cells expressing the Gp 170 protein. Anticancer research. 1992;12(2):495-499.

65. Landen CN, Merritt WM, Mangala LS, et al. Intraperitoneal delivery of liposomal siRNA for therapy of advanced ovarian cancer. Cancer biology & therapy. 2006;5(12):1708-1713.

66. Sadzuka Y, Hirama R, Sonobe T. Effects of intraperitoneal administration of liposomes and methods of preparing liposomes for local therapy. Toxicology letters. 2002 Jan 25;126(2):83-90.

Figure 1. Effect of pH of the dispersion medium on peptide in vitro release (A), effect of peptide loading on peptide in vitro release (B) and effects of DOX addition on peptide in vitro release (C). Values are mean ± SD for (n = 3).
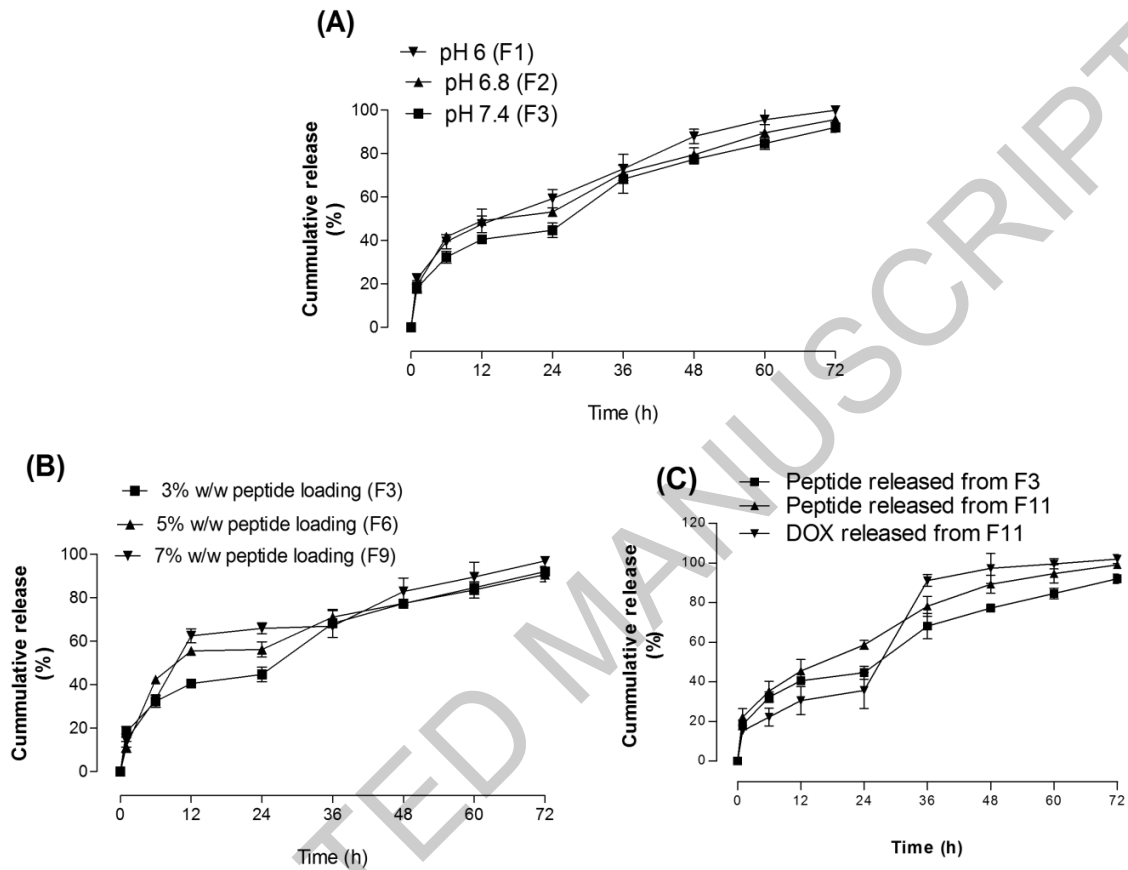

Figure 2. TEM images of dual-loaded liposome (F11) after preparation (A). Particle size measurements of the F11 liposome formulation over 28 days of storage at 4oC. Values are mean ± SD for (n = 3). *p < 0.05 compared to day 0 (B).
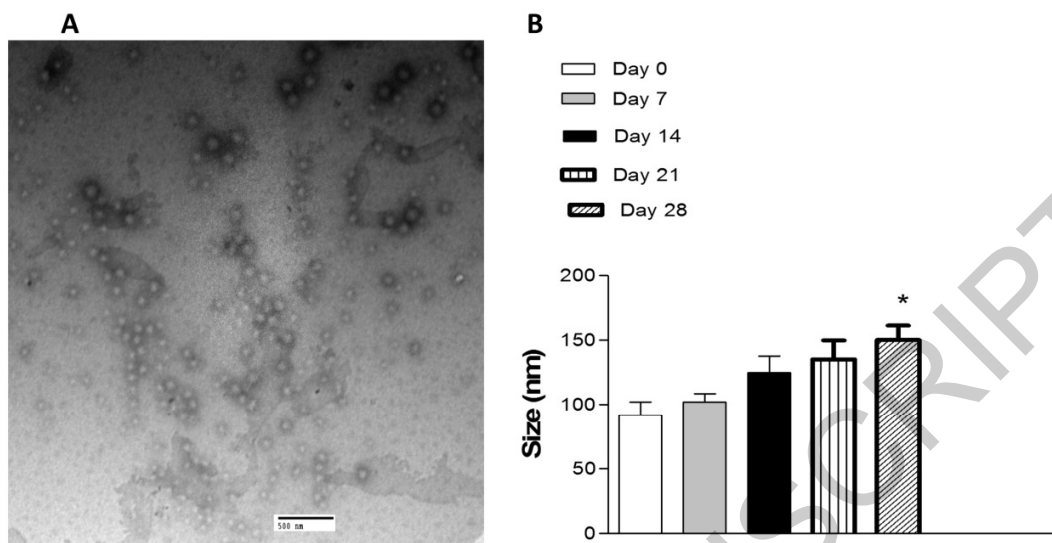
Figure 3. Cell viability results of different doses of peptide-loaded liposomes in MDA-MB-231 (A), MCF-7 (B) and A549 (C) after 24, 48 and 72 h.
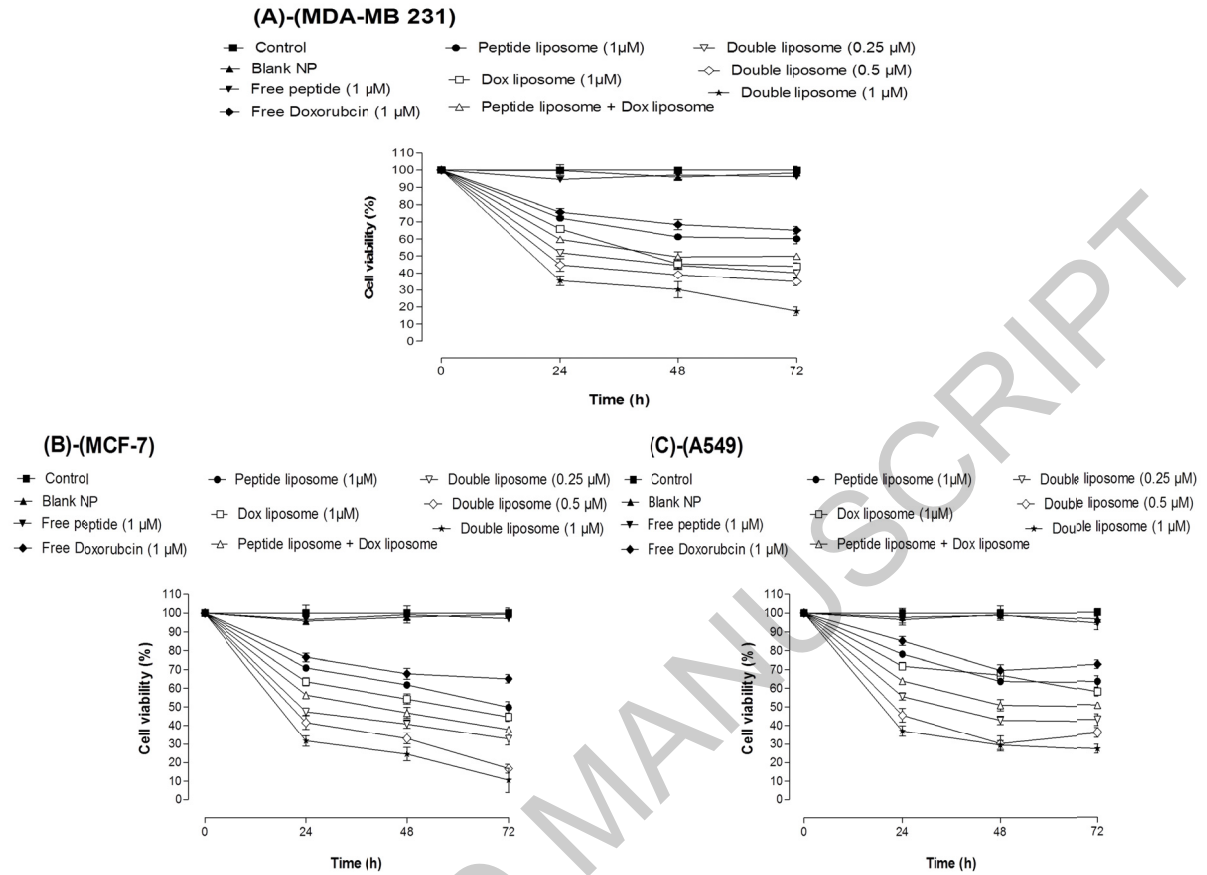
(A)-(MDA-MB 231)

- ■ Control
- ▲ Blank NP
- ▼ Free peptide (1 µM)
- ◆ Free Doxorubcir (1 µM)
- ● Peptide liposome (1µM)
- □ Dox liposome (1µM)
- △ Peptide liposome + Dox liposome
- ▽ Double liposome (0.25 µM)
- ◇ Double liposome (0.5 µM)
- ★ Double liposome (1 µM)

(B)-(MCF-7)

- ■ Control
- ▲ Blank NP
- ▼ Free peptide (1 µM)
- ◆ Free Doxorubcin (1 µM)
- ● Peptide liposome (1µM)
- □ Dox liposome (1µM)
- △ Peptide liposome + Dox liposome
- ▽ Double liposome (0.25 µM)
- ◇ Double liposome (0.5 µM)
- ★ Double liposome (1 µM)

(C)-(A549)

- ■ Control
- ▲ Blank NP
- ▼ Free peptide (1 µM)
- ◆ Free Doxorubcin (1 µM)
- ● Peptide liposome (1µM)
- □ Dox liposome (1µM)
- △ Peptide liposome + Dox liposome
- ▽ Double liposome (0.25 µM)
- ◇ Double liposome (0.5 µM)
- ★ Double liposome (1 µM)

Figure 4. % of RAN mRNA expression in MDA-MB-231 treated cells with Dox. 1 µM and 1.3µM at 6,12 and 24 hours- 6(A). % of RAN mRNA expression at 24 hours(B). Values are mean ± SD for (n=3). *p < 0.05, **p < 0.01, ***p < 0.001 compared with blank liposome, ???P<0.001 compared with 6 and 12 hours for (A) and **p < 0.01, ***p < 0.001 compared with blank liposome, ???P<0.001 compared DOX liposome (1 and 1.3 µM) for (B).
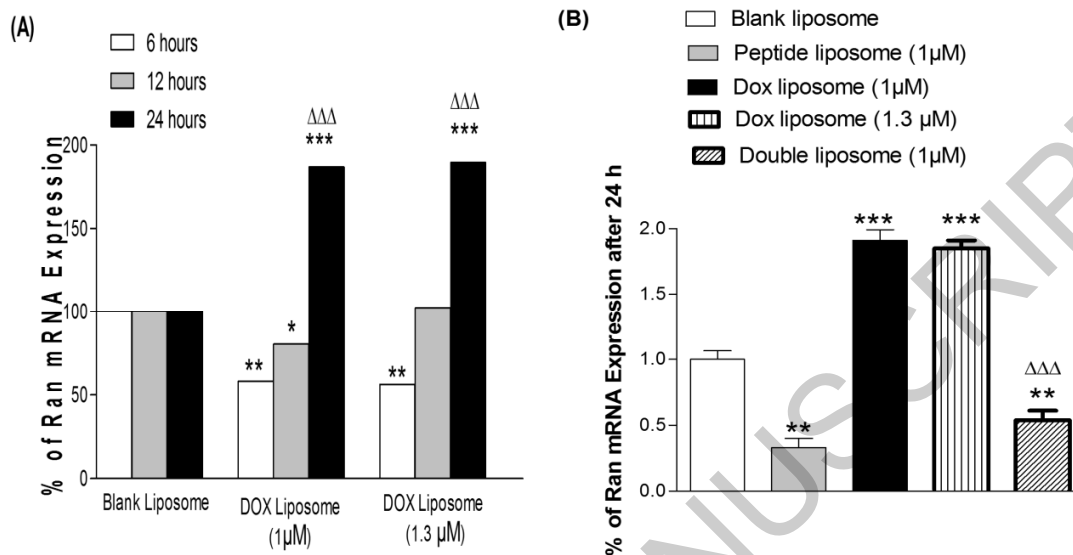
Figure 5. Tumor volume recorded for the studied animal groups treated with different peptide-loaded liposome. Results were reordered every 2 days from the 1st day of the treatment to the last record at the 16th day (the end of the experiment). Values are mean ± SEM for (n = 6).
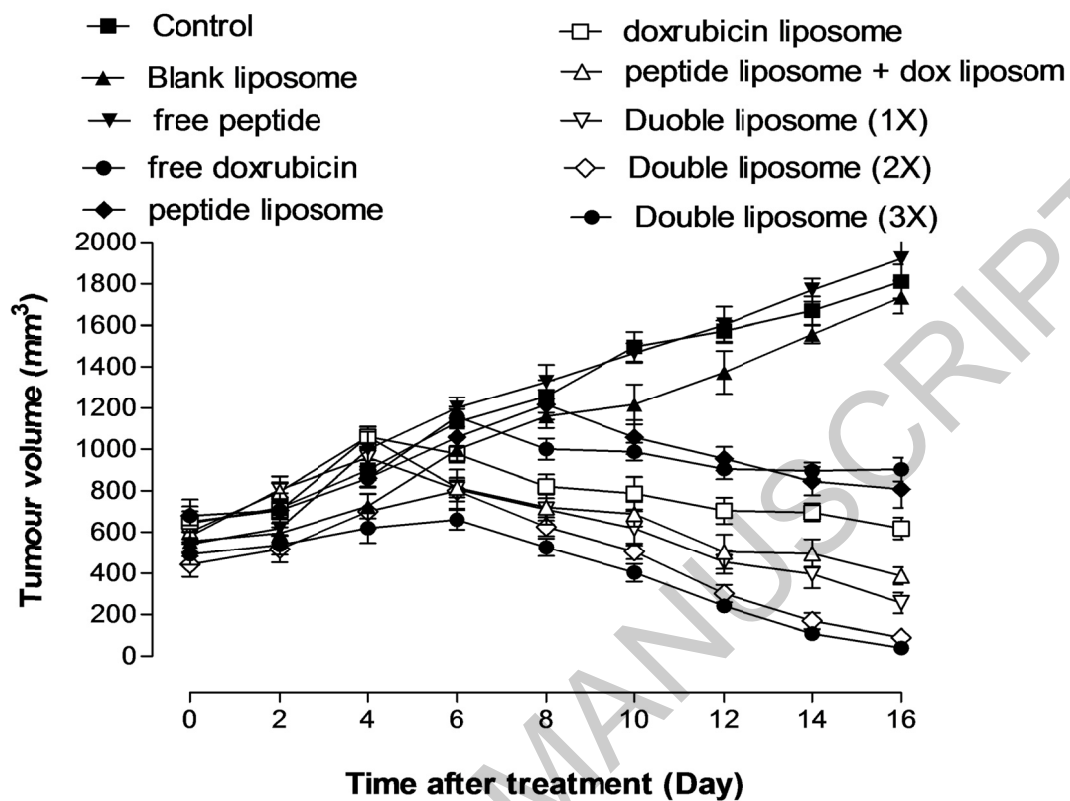
Figure 6. Percentage tumor growth inhibition (% TGI) in animals treated with different peptide-loaded liposome. *P<0.05, **P<0.01, ***P<0.001 compared with control group. ?P<0.05, ?? P<0.01, ???P<0.001 compared with free drugs.

Legend:
- ▭ Blank liposome
- ▮ free peptide
- ⊞ free doxrubicin
- ▨ peptide liposome
- ▥ doxrubicin liposome
- ⊠ peptide liposome + dox liposom
- ⊟ Double liposome (1X)
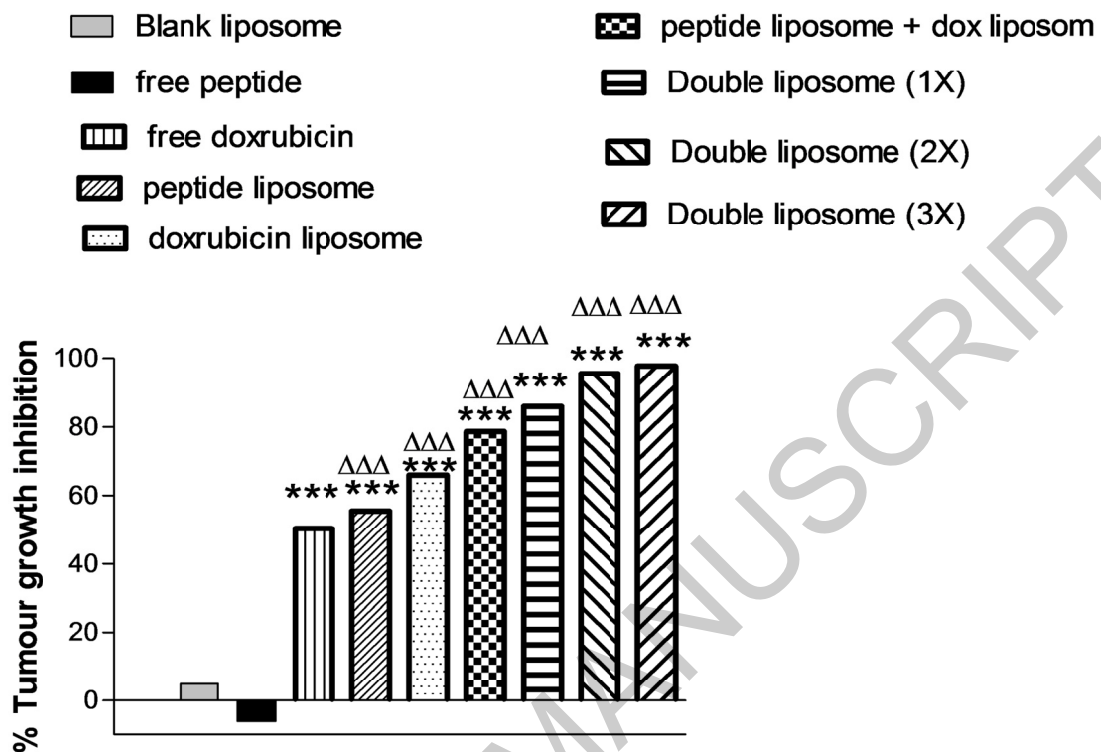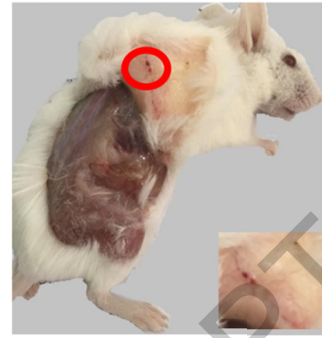- ◲ Double liposome (2X)
- ◿ Double liposome (3X)

Figure 7. Photographs of excised tumors from animals treated with different peptide-loaded liposome.
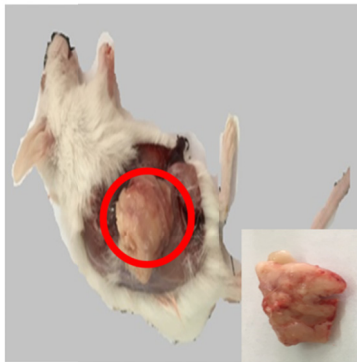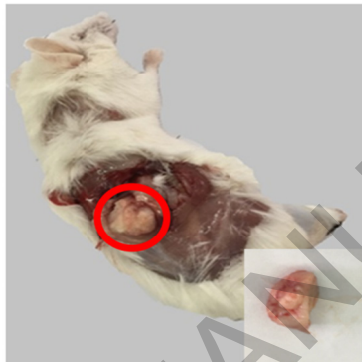
Control

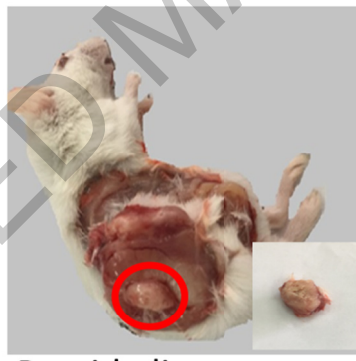Peptide liposome

Double liposome (2X)

Blank liposome

Doxorubicin liposome

Double liposome (3X)

Free peptide

Peptide liposome +
doxorubicin liposome

Free doxorubicin

Double liposome (1X)

Figure 8. Tumor weight of studied animal groups treated with different peptide-loaded liposome, after the end of the experiment. Values are mean ± SEM for (n = 6). *P<0.05, **P<0.01, ***P<0.001 compared with control group. ?P<0.05, ??P<0.01, ???P<0.001 compared with free drugs.
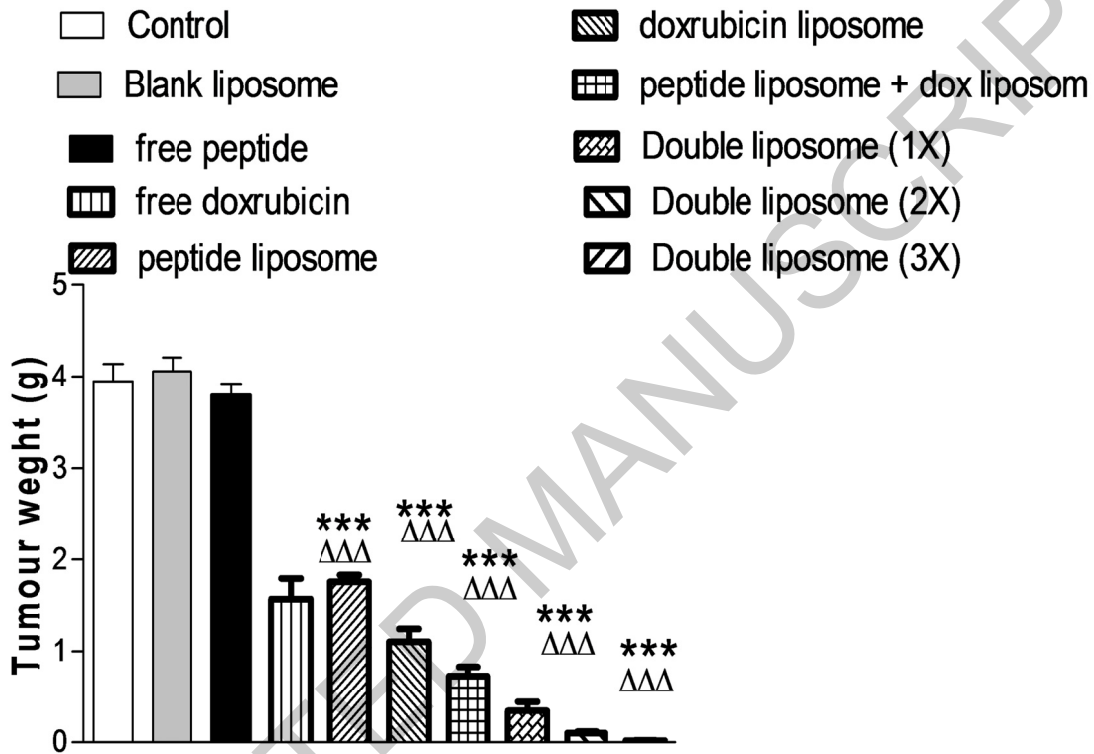

Figure 9. Body weight of studied animal groups treated with different prepared liposome in table 2, after the end of the experiment, Values are mean ± SEM for (n = 6).*P<0.05, **P<0.01, ***P<0.001 compared with control group. ?P<0.05, ??P<0.01, ???P<0.001 compared with free DOX.
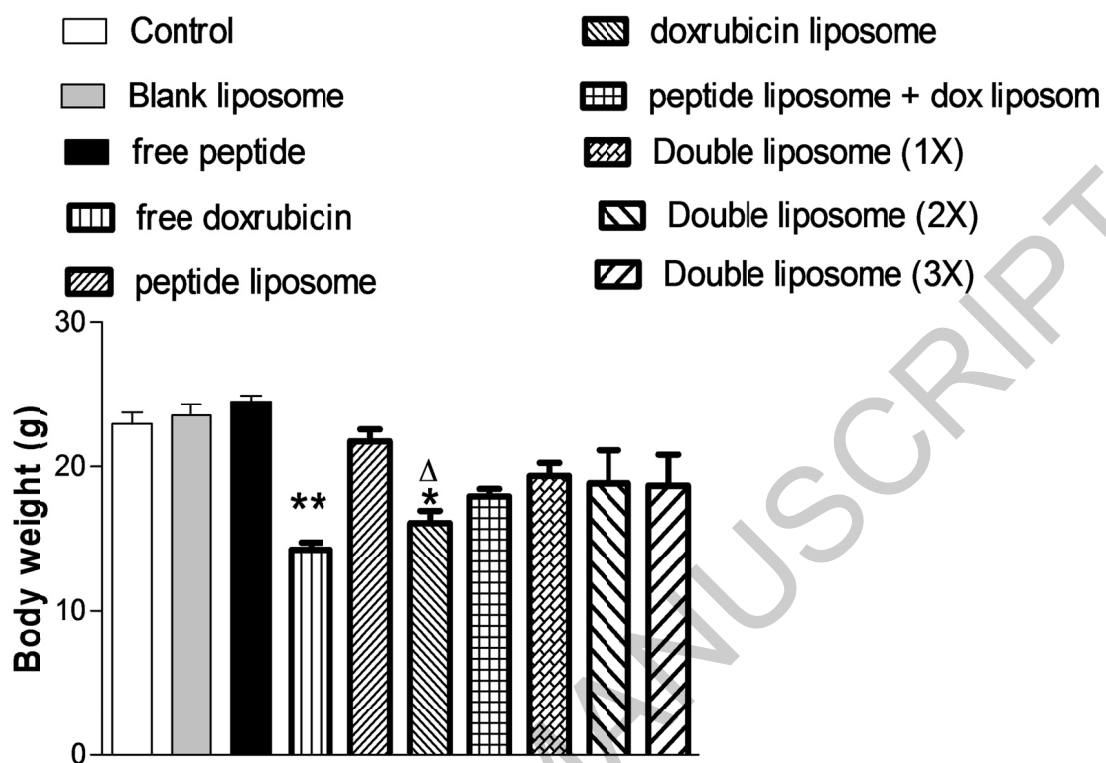
Table 1. Process variables for peptide-loaded, DOX-loaded and dual-loaded liposomes and corresponding identifiers

Formulation identifier	Encapsulated drug	pH of dispersion media	Drug loading
F1	NT 3-12 peptide	6.0	3% w/w
F2	NT 3-12 peptide	6.8	3% w/w
F3	NT 3-12 peptide	7.4	3% w/w
F4	NT 3-12 peptide	6.0	5% w/w
F5	NT 3-12 peptide	6.8	5% w/w
F6	NT 3-12 peptide	7.4	5% w/w
F7	NT 3-12 peptide	6.0	7% w/w
F8	NT 3-12 peptide	6.8	7% w/w
F9	NT 3-12 peptide	7.4	7% w/w
F10	DOX	7.4	5% w/w
F11	NT 3-12 peptide and DOX	7.4	3% w/w of peptide and 5% w/w of DOX

ACCEPTED MANUSCRIPT

Table 2. Physicochemical characterizations of peptide-loaded, DOX-loaded and dual-loaded liposomes

Formulation identifier	Size (nm)	Zeta potential (mV)	% Encapsulation Efficiency
F1	138.47 ± 21.11	-27.55 ± 3.44	52.13 ± 7.96
F2	119.50 ± 10.69	-28.11 ± 5.69	54.17 ± 5.89
F3	$80.55 \pm 11.23^{**}$	-26.21 ± 2.58	$93.15 \pm 6.10^{***}$
F4	185.56 ± 16.33	-29.11 ± 4.23	41.25 ± 4.58
F5	177.22 ± 13.44	-26.39 ± 3.12	43.47 ± 6.11
F6	116.75 ± 11.99 $^{\Delta}$	-25.22 ± 3.69	72.36 ± 7.89 $^{\Delta}$
F7	244.88 ± 9.78	-27.16 ± 4.55	32.15 ± 4.19
F8	226.75 ± 13.74	-28.14 ± 5.37	30.36 ± 9.74
F9	127.51 ± 14.35 $^{\Delta\Delta}$	-28.21 ± 1.36	64.78 ± 2.14 $^{\Delta\Delta}$
F10	105.66 ± 17.95	-29.64 ± 4.87	83.77 ± 8.85
F11	91.75 ± 18.27	-20.23 ± 1.54 $^{\Delta}$	85.12 ± 7.68 for peptide 80.60 ± 5.36 for DOX

Values were represented as mean $\pm$ SD (n=3), $^{**}p < 0.01$, $^{***}p < 0.001$ compared with (F1), $^{\Delta} p < 0.05$, $^{\Delta\Delta} p < 0.01$, compared with (F3).

Table 3. Study design and animal treatment protocol

Group No	Group ID	Intraperitoneal treatment
1	Control	saline
2	Blank Liposomes	blank liposomes
3	Free peptide	free peptide (10 mg kg^{-1})
4	Free DOX	free DOX (5 mg kg^{-1})
5	Peptide-loaded liposomes	peptide-loaded liposomes (10 mg kg^{-1})
6	DOX-loaded liposomes	DOX-loaded liposomes (5 mg kg^{-1})
7	Peptide liposome+ DOX liposome	Peptide-loaded liposomes (10 mg kg^{-1}) and DOX-loaded liposomes (5 mg kg^{-1}).
8	Dual-loaded liposomes (1X)	dual-loaded liposomes (peptide 5 mg kg^{-1} and DOX 2.5 mg kg^{-1}).
9	Dual-loaded liposomes (2X)	dual-loaded liposomes (peptide 10mg kg^{-1} and DOX 5 mg kg^{-1}).
10	Dual-loaded liposomes (3X)	dual-loaded liposomes (peptide 15 mg kg^{-1} and DOX 7.5 mg kg^{-1}).

Table 4. Effect of peptide-loaded liposomes on cardiac MDA and serum level of cardiac biomarkers

Group ID	Cardiac MDA (nmole per g tissue)	LDH (uKat l^{-1})	CK-MB (uKat l^{-1})
Normal animals	90.25± 28.16	3.05 ± 0.297	0.31± 0.11
Control	99.654 ± 17.265	3.99 ± 0.458	0.35 ± 0.045
Blank Liposome	105.23 ± 11.236	4.125 ± 0.998	0.42 ± 0.031
Free peptide	109.774 ± 14.265	3.751 ± 0.898	0.405 ± 0.15
Free DOX	145.998 ± 21.45**	6.025 ± 0.108**	1.52 ± 0.13**
Peptide liposome	111.244 ± 9.265	4.139 ± 0.058	0.39 ± 0.05
DOX liposome	134.23 ± 19.556*	5.725 ± 0.098*	1.29 ± 0.45*
Peptide liposome+ DOX liposome	139.794 ± 7.265*	4.99 ± 0.968*	1.15 ± 0.65**
Double-loaded liposome (1X)	105.023 ± 8.996	4.105 ± 0.218	0.79 ± 0.33
Double-loaded liposome (2X)	112.56 ± 19.88	4.34 ± 0.83	0.82 ± 0.48
Double-loaded liposome (3X)	117.32 ± 21.452	5.05 ± 0.79	0.69 ± 0.52

Values are mean ± SEM (n = 6).*p < 0.05, **p < 0.01 compared to control group